Radiation Thickness, Collisional Thickness, and Most Probable Collisional Energy Loss for E08-027

Ryan Zielinski
University of New Hampshire
rbziel@jlab.org

November 2, 2016

Abstract

The external radiative corrections depend on the thickness of material before and after scattering. This note is a catalog of radiation lengths and materials for E08-027. It also includes a calculation of the collisional thicknesses and most probable energy loss values for materials in the beam path.

Contents

List of Figures

List of Tables

Z -	**atom**	A amu	σ_{rad} barns	X_0 g/cm^2
1	H	1.00794	0.02655	63.0435
2	He	4.00260	0.07047	94.3224
4	Be	9.01218	0.22956	65.1900
5	B	10.81100	0.34073	52.6868
6	C	12.01070	0.46711	42.6969
7	N	14.00670	0.61226	37.9879
8	O	15.99940	0.77597	34.2382
11	Na	22.98977	1.37637	27.7362
12	Mg	24.30500	1.61235	25.0315
13	Al	26.98154	1.86596	24.0112
14	Si	28.08550	2.13706	21.8231
19	K	39.09830	3.74958	17.3151
20	Ca	40.07800	4.12249	16.1434
33	As	74.92160	10.41949	11.9401
38	Sr	87.62000	13.51897	10.7624
56	Ba	137.32700	27.45233	8.3066

material	ammonia	Kapton
formula	$^{14}NH_3$	$(C_{22}H_{10}N_2O_5)_n$
C by wt.	-	0.691133
O by wt.	-	0.209235
N by wt.	0.822453	0.073270
H by wt.	0.177547	0.026362
X_0 (g/cm^2)	40.87	40.5761

Table 1: Radiation lengths for atomic species and composite materials. [2].

1 Introduction and Relevant Formulas

The use of an accelerated and charged probe in electron scattering experiments causes real photon bremsstrahlung emission as the electron scatters from the target and interacts with the material it traverses before, after and within the target. The bremsstrahlung emission resulting from material in the beam path is characterized by the material's radiation length. The radiation length of a material is defined as the thickness required for an electron to lose 1-1/e of its energy as it travels through the material. For a single atomic species, the radiation length in mass per unit "area" is given by

$$X_0 = \frac{A}{N_A \sigma_{\mathrm{rad}}(Z)}\,, \tag{1}$$

and for for a composite material it is given by the sum

$$X_0^{-1} = \sum_k \frac{w_k N_A \sigma_{\mathrm{rad}}(Z_k)}{A_k} = \sum_k \frac{w_k}{X_0^k}\,, \tag{2}$$

where w_k represents the mass fraction for the k-th component of the total mass of the composite material. The radiation lengths used in this analysis are shown in Table 1. To take into account differences in the physical thicknesses and densities of the various beam line materials, each material's radiation length is weighted by the thickness and density and then summed,

$$t = \sum_j \frac{\rho_j \ell_j}{X_0^j}\,, \tag{3}$$

where the sum over j runs over each composite material with physical thickness ℓ_j and mass density ρ_j. The weighted sum is referred to as the radiation thickness (see Ref [1], [2]).

In addition to bremsstrahlung emission, it's possible for the electron to elastically scatter with atomic electrons from the materials in the beam path. The energy lost to a single ionizing collision is given by [3]

$$\frac{\xi}{\rho x} = \frac{Za}{A\beta^2} \tag{4}$$

$$a = 2\pi N_A r_e^2 m_e c^2 = 0.15353747 \text{ MeV} \cdot \frac{\text{cm}^2}{\text{mol}} \tag{5}$$

$$\beta = \frac{v}{c} = \frac{pc}{E}\,, \tag{6}$$

where ρ and x are the materials mass density and thickness, N_A is Avogadro's numbers and r_e is the classical electron radius. The effects of the ionization of many atoms is represented by adjusting the incoming and outgoing electron energies such that

$$E_{\text{inc.}} = E_{\text{beam}} - \Delta_s \tag{7}$$

$$E_{\text{fin.}} = E' + \Delta_p \tag{8}$$

$$E' \simeq p_{\text{spect}}\,, \tag{9}$$

where $\Delta_{s,p}$ is energy loss due to the ionizing collisions; for a highly relativistic electron $p \simeq E$. The form of $\Delta_{s,p}$ is given by [4]

$$\frac{\Delta}{\rho x} = \left(\frac{\xi}{\rho x}\right)\left[2\log\left(\frac{pc}{I}\right) - \delta(X) + g\right] \tag{10}$$

$$\bar{g} = \log(\gamma - 1) - F(\gamma) \qquad \text{mean energy loss (Bethe} - \text{Bloch)} \tag{11}$$

$$g_{\text{mp}} = \log\left[\frac{2\xi}{m_e c^2}\right] - \beta^2 + 0.198 \qquad \text{most probable (Landau)} \tag{12}$$

$$F(\gamma) = \left[1 + \frac{2}{\gamma} - \frac{1}{\gamma^2}\right]\log(2) - \frac{1}{8}\left[1 - \frac{1}{\gamma}\right]^2 - \frac{1}{\gamma^2} \tag{13}$$

$$\gamma = \frac{1}{\sqrt{1-\beta^2}} = \frac{E}{m_e c^2}\,, \tag{14}$$

where I is the mean excitation energy of the material and $\delta(X)$ is the density correction. The density correction is given as [5, 6]

$$\delta(X) = \left\{\begin{array}{ll} \delta\left(X_0^\delta\right) \times 10^{2\left(X - X_0^\delta\right)} & X \leq X_0^\delta \\ 2\log(10)\left(X - X_a^\delta\right) + a_\delta\left(X_1^\delta - X\right)^{m_\delta} & X_0^\delta < X < X_1^\delta \\ 2\log(10)\left(X - X_a^\delta\right) & X \geq X_1^\delta \end{array}\right\} \tag{15}$$

$$X = \log_{10}\left(\frac{p}{m_e c}\right) \tag{16}$$

$$X_a^\delta = \frac{-C_\delta}{2\log(10)} \tag{17}$$

$$a_\delta = \frac{\delta\left(X_0^\delta\right) + 2\log(10)\left(X_a^\delta - X_0^\delta\right)}{\left(X_1^\delta - X_0^\delta\right)^{m_\delta}} \tag{18}$$

where C_δ, X_0^δ, X_1^δ, m_δ and $\delta(X_0^\delta)$ are material dependent and are shown in Table 2 and Table 3. If the density of a material is different than that listed in Table 2 and Table 3, then the density correction parameters are adjusted as follows

$$X_a^{\delta\prime} = X_a^\delta - \frac{1}{2}\log_{10}\left(\frac{\text{N}}{\text{N}_0}\right) \tag{19}$$

$$X_0^{\delta\prime} = X_0^\delta - \frac{1}{2}\log_{10}\left(\frac{\text{N}}{\text{N}_0}\right) \tag{20}$$

$$X_1^{\delta\prime} = X_1^\delta - \frac{1}{2}\log_{10}\left(\frac{\text{N}}{\text{N}_0}\right) \tag{21}$$

where N_0 is the density from the table and N is the desired density [1].

	Z/A	I eV	I' (g) eV	I' (l/s) eV	ρ g/cm^3	$-C$	X_0	X_1	a	m	$\delta(X_0)$
H	0.9922	19.2	19.2	19.2	8.3748E−05	9.5835	1.8639	3.2718	0.14095	5.7273	0.00
He	0.4997	41.8	41.8	47.2	1.6632E−04	11.1393	2.2017	3.6122	0.13443	5.8347	0.00
Be	0.4438	63.7	63.7	72.0	1.8480E+00	2.7847	0.0592	1.6922	0.76146	2.4339	0.14
B	0.4625	76.0	76.0	85.9	2.3700E+00	2.8477	0.0305	1.9688	0.56221	2.4512	0.14
C	0.4995	78.0	70.0	81.0	2.0000E+00	2.9925	-0.0351	2.4860	0.20489	3.0036	0.10
N	0.4998	82.0	82.0	82.0	1.1653E−03	10.5400	1.7378	4.1323	0.15955	3.2125	0.00
O	0.5000	95.0	97.0	106.0	1.3315E−03	10.7004	1.7541	4.3213	0.11778	3.2913	0.00
Na	0.4785	149.0	149.0	168.4	9.7100E−01	5.0526	0.2880	3.1962	0.07608	3.6452	0.08
Mg	0.4937	156.0	156.0	176.3	1.7400E+00	4.5297	0.1499	3.0668	0.08162	3.6166	0.08
Al	0.4818	166.0	166.0	187.6	2.6989E+00	4.2395	0.1708	3.0127	0.07934	3.6345	0.12
Si	0.4985	173.0	173.0	195.5	2.3300E+00	4.4351	0.2014	2.8715	0.14840	3.2546	0.14
K	0.4860	190.0	190.0	214.7	8.6200E−01	5.6423	0.3851	3.1724	0.20027	2.9233	0.10
Ca	0.4990	191.0	191.0	215.8	1.5500E+00	5.0396	0.3228	3.1191	0.15475	3.0745	0.14
As	0.4405	347.0	347.0	392.1	5.7300E+00	5.0510	0.1767	3.5702	0.06725	3.4176	0.08
Sr	0.4337	366.0	366.0	413.6	2.5400E+00	5.9867	0.4585	3.6778	0.07058	3.4435	0.14
Ba	0.4078	491.0	491.0	554.8	3.5000E+00	6.3153	0.4190	3.4547	0.18267	2.8906	0.14

Table 2: Density correction parameters for a single atomic species [6]. The densities are given for the natural form of the element (gas, diatomic gas, liquid, solid) at 1 atm and 20°C.

	Z/A	I eV	ρ g/cm^3	$-C$	X_0	X_1	a	m
$^{14}NH_3$	0.5972	53.69	8.2602E−04	9.8763	1.6822	4.1158	0.08315	3.6464
kapton	0.5126	79.60	1.4200E+00	3.3497	0.1509	2.5631	0.15971	3.1921

Table 3: Density correction parameters for composite materials. For all these materials $\delta(X_0) = 0$. The density of ammonia listed here is for gaseous ammonia.

2 Materials in the Beam Path

The materials encountered by the electron before and after scattering are shown in Figure 2. The incident electrons exit the beam pipe through a beryllium window and proceed through a helium bag before entering the aluminum scattering chamber. The scattering chamber is held under vacuum and contains the Helmoltz coils of the target magnetic field and the bottom of the target refrigerator. The bottom of the refrigerator or "nose" is made out of aluminum and keeps the target materials immersed in $\sim$1K liquid helium.

The E08-027 target stick holds several different targets, shown in Figure 1. Starting from the left, there is a carbon foil, dummy cell, production target cell filled with ammonia beads, two empty holes for additional carbon foils and CH_2 targets, and finally, another production target cell. The dummy and production cells have thin aluminum end caps. The target cell has a radius of 1.361 cm and a length of 2.827 (1.295 for the short production cell) cm. The amount of liquid helium versus frozen ammonia beads in the target cell is dependent on the packing fraction of the ammonia beads. For this analysis the packing fraction was assumed to be 0.55 and the lengths of the helium and ammonia in the target cells was scaled accordingly. The NMR coil is not considered in the radiation lengths. The separation between radiation thicknesses before and after scattering is halfway through the target material. This does not coincide with the center of the target cup for the carbon foil targets.

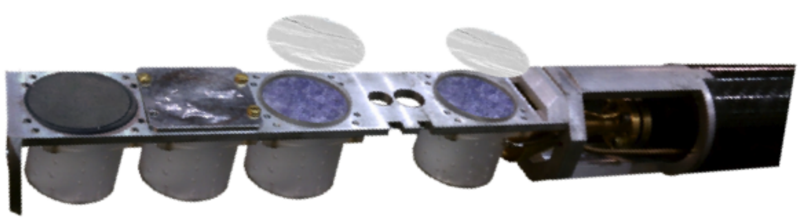

Figure 1: Target stick for g2p.

The scattered electrons exit through the other side of the aluminum target nose and continue through the vacuum of the scattering chamber. After leaving the scattering chamber, they continue onwards to the septa magnet and ultimately the kapton entrance windows of the high resolution spectrometers. To prevent hazardous ionization of the air, a helium bag starts at the exit of the scattering chamber and ends at the entrance of the spectrometers, surrounding the bores of the septa magnets.

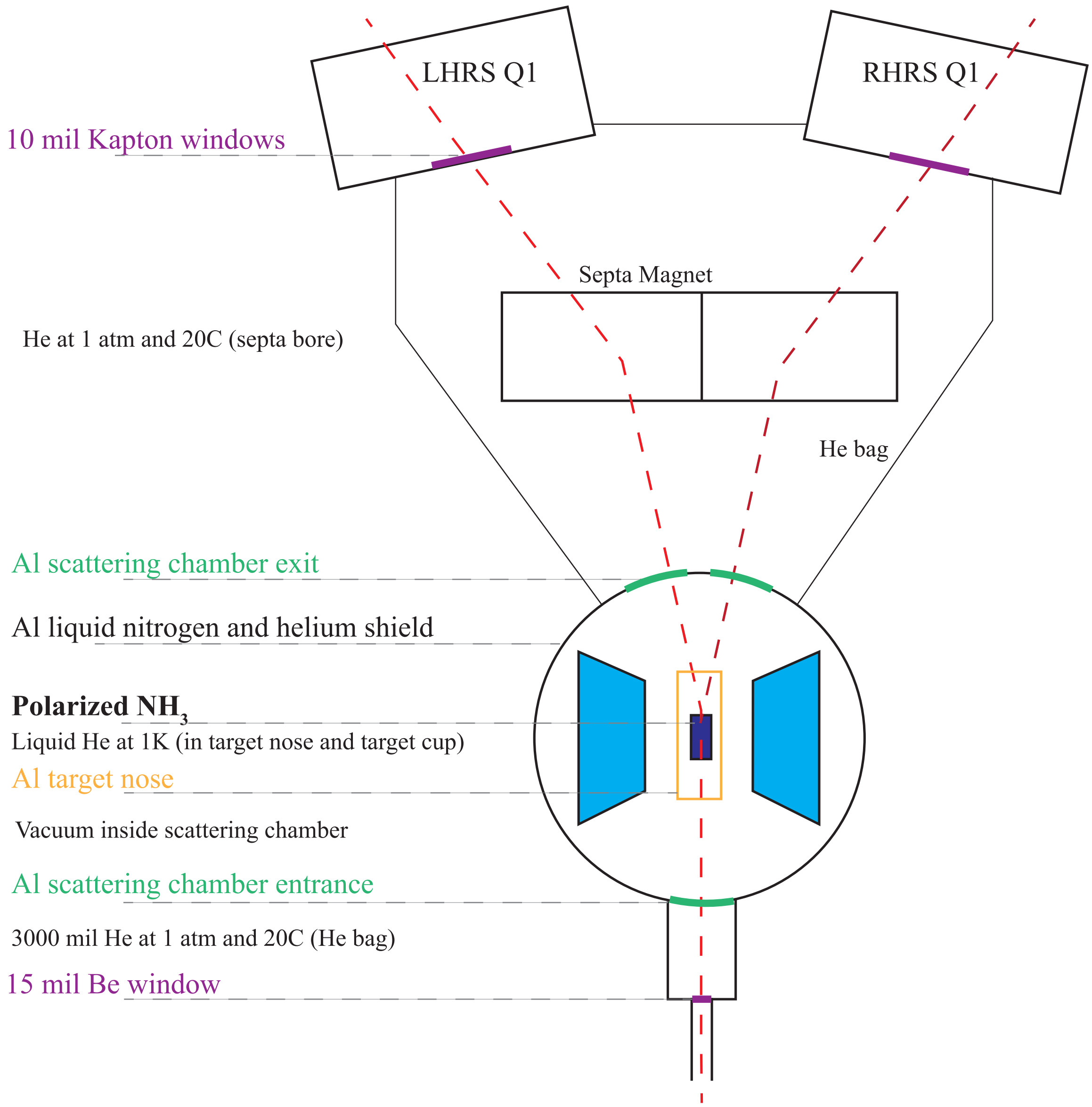

Figure 2: Hall A Layout for g2p.

material	X_0	ρ	$\bar{X}_0$	ℓ	t	**fraction of tot**
	g/cm^2	g/cm^3	cm	cm	–	–
Beryllium Window	65.1900	1.848E+00	3.528E+01	3.810E−01	1.081E−03	0.0481
Helium Bag	94.3224	1.786E−04	5.281E+05	7.620E+00	1.443E−05	0.0006
Scat. Chamber	24.0112	2.700E+00	8.893E+00	1.780E−02	2.002E−03	0.0890
LN_2 Shield	24.0112	2.700E+00	8.893E+00	3.800E−03	4.284E−04	0.0190
4K Shield	24.0112	2.700E+00	8.893E+00	1.300E−03	1.462E−04	0.0065
Target Nose	24.0112	2.700E+00	8.893E+00	1.270E−02	1.428E−03	0.0635
LHe in Nose	94.3224	1.450E−01	6.505E+02	4.369E−01	6.716E−04	0.0299
Target End Cap	24.0112	2.700E+00	8.893E+00	1.800E−03	1.999E−04	0.0089
LHe Target Cup	94.3224	1.450E−01	6.505E+02	6.361E−01	9.779E−04	0.0435
Solid NH_3	40.8721	8.170E−01	5.003E+01	7.774E−01	1.554E−02	0.6910
Total Before	2.249E−02					
Solid NH_3	40.8721	8.170E−01	5.003E+01	7.774E−01	1.554E−02	0.5905
LHe Target Cup	94.3224	1.450E−01	6.505E+02	6.361E−01	9.779E−04	0.0372
Target End Cap	24.0112	2.700E+00	8.893E+00	1.800E−03	1.999E−04	0.0076
LHe in Nose	94.3224	1.450E−01	6.505E+02	4.369E−01	6.716E−04	0.0255
Target Nose	24.0112	2.700E+00	8.893E+00	1.270E−02	1.428E−03	0.0543
4K Shield	24.0112	2.700E+00	8.893E+00	1.300E−03	1.462E−04	0.0056
LN_2 Shield	24.0112	2.700E+00	8.893E+00	3.800E−03	4.284E−04	0.0163
Scat. Chamber	24.0112	2.700E+00	8.893E+00	5.080E−02	5.712E−03	0.2170
Helium Bag	94.3224	1.786E−04	5.281E+05	1.709E+02	3.236E−04	0.0123
Kapton Window	40.5761	1.420E+00	2.857E+01	2.540E−02	8.889E−04	0.0338
Total After	2.632E−02					

Table 4: Radiation thicknesses before and after scattering for the normal g2p production target.

3 Results

The lengths of the materials in this analysis are from Ref. [7], and the results are shown in Table **??** through Table 15. The results apply to all production, packing fraction and dilution runs. For optics runs one has to be careful because they were frequently run without liquid helium in the nose. The density of liquid helium plateaus below 2K, so a constant density of 0.145 g/cm^3 is assumed.

material	ρ	ℓ	ξ	mp	dE
	g/cm^3	cm	MeV	MeV	MeV
Beryllium Window	1.848E+00	3.810E−01	4.803E−03	0.077	0.136
Helium Bag	1.786E−04	7.620E+00	1.044E−04	0.002	0.004
Scat. Chamber	2.700E+00	1.780E−02	3.555E−03	0.054	0.099
LN_2 Shield	2.700E+00	3.800E−03	7.610E−04	0.010	0.021
4K Shield	2.700E+00	1.300E−03	2.596E−04	0.003	0.007
Target Nose	2.700E+00	1.270E−02	2.537E−03	0.038	0.070
LHe in Nose	1.450E−01	4.369E−01	4.860E−03	0.090	0.149
Target End Cap	2.700E+00	1.800E−03	3.551E−04	0.005	0.010
LHe Target Cup	1.450E−01	6.361E−01	7.076E−03	0.138	0.217
Solid NH_3	8.170E−01	7.774E−01	5.824E−02	1.148	1.675
Total Before			8.255E−02	1.565	2.387
Solid NH_3	8.170E−01	7.774E−01	5.824E−02	1.148	1.675
LHe Target Cup	1.450E−01	6.361E−01	7.076E−03	0.138	0.217
Target End Cap	2.700E+00	1.800E−03	3.551E−04	0.005	0.010
LHe in Nose	1.450E−01	4.369E−01	4.860E−03	0.090	0.149
Target Nose	2.700E+00	1.270E−02	2.537E−03	0.038	0.070
4K Shield	2.700E+00	1.300E−03	2.596E−04	0.003	0.007
LN_2 Shield	2.700E+00	3.800E−03	7.610E−04	0.010	0.021
Scat. Chamber	2.700E+00	5.080E−02	1.015E−02	0.165	0.282
Helium Bag	1.786E−04	1.709E+02	2.342E−03	0.057	0.087
Kapton Window	1.420E+00	2.540E−02	2.839E−03	0.044	0.080
Total After			8.942E−02	1.698	2.599

Table 5: Energy loss before and after scattering for the normal g2p production target.

material	X_0 g/cm^2	ρ g/cm^3	$\bar{X}_0$ cm	ℓ cm	t –	**fraction of tot** –
Beryllium Window	65.1900	1.848E+00	3.528E+01	3.810E−01	1.081E−03	0.0799
Helium Bag	94.3224	1.786E−04	5.281E+05	7.620E+00	1.443E−05	0.0011
Scat. Chamber	24.0112	2.700E+00	8.893E+00	1.780E−02	2.002E−03	0.1478
LN_2 Shield	24.0112	2.700E+00	8.893E+00	3.800E−03	4.284E−04	0.0316
4K Shield	24.0112	2.700E+00	8.893E+00	1.300E−03	1.462E−04	0.0108
Target Nose	24.0112	2.700E+00	8.893E+00	1.270E−02	1.428E−03	0.1055
LHe in Nose	94.3224	1.450E−01	6.505E+02	4.369E−01	6.716E−04	0.0496
Target End Cap	24.0112	2.700E+00	8.893E+00	1.800E−03	1.999E−04	0.0148
LHe Target Cup	94.3224	1.450E−01	6.505E+02	2.914E−01	4.479E−04	0.0331
Solid NH_3	40.8721	8.170E−01	5.003E+01	3.562E−01	7.119E−03	0.5258
Total Before	1.354E−02					
Solid NH_3	40.8721	8.170E−01	5.003E+01	3.562E−01	7.119E−03	0.3610
LHe Target Cup	94.3224	1.450E−01	6.505E+02	2.914E−01	4.479E−04	0.0227
Target End Cap	24.0112	2.700E+00	8.893E+00	1.800E−03	1.999E−04	0.0101
LHe in Nose	94.3224	1.450E−01	6.505E+02	1.969E+00	3.027E−03	0.1535
Target Nose	24.0112	2.700E+00	8.893E+00	1.270E−02	1.428E−03	0.0724
4K Shield	24.0112	2.700E+00	8.893E+00	1.300E−03	1.462E−04	0.0074
LN_2 Shield	24.0112	2.700E+00	8.893E+00	3.800E−03	4.284E−04	0.0217
Scat. Chamber	24.0112	2.700E+00	8.893E+00	5.080E−02	5.712E−03	0.2897
Helium Bag	94.3224	1.786E−04	5.281E+05	1.709E+02	3.236E−04	0.0164
Kapton Window	40.5761	1.420E+00	2.857E+01	2.540E−02	8.889E−04	0.0451
Total After	1.972E−02					

Table 6: Radiation thicknesses before and after scattering for the thin g2p production target.

material	ρ g/cm^3	ℓ cm	ξ MeV	mp MeV	dE MeV
Beryllium Window	1.848E+00	3.810E−01	4.803E−03	0.077	0.136
Helium Bag	1.786E−04	7.620E+00	1.044E−04	0.002	0.004
Scat. Chamber	2.700E+00	1.780E−02	3.555E−03	0.054	0.099
LN_2 Shield	2.700E+00	3.800E−03	7.610E−04	0.010	0.021
4K Shield	2.700E+00	1.300E−03	2.596E−04	0.003	0.007
Target Nose	2.700E+00	1.270E−02	2.537E−03	0.038	0.070
LHe in Nose	1.450E−01	4.369E−01	4.860E−03	0.090	0.149
Target End Cap	2.700E+00	1.800E−03	3.551E−04	0.005	0.010
LHe Target Cup	1.450E−01	2.914E−01	3.241E−03	0.061	0.099
Solid NH_3	8.170E−01	3.562E−01	2.668E−02	0.505	0.767
Total Before			4.715E−02	0.845	1.362
Solid NH_3	8.170E−01	3.562E−01	2.668E−02	0.505	0.767
LHe Target Cup	1.450E−01	2.914E−01	3.241E−03	0.061	0.099
Target End Cap	2.700E+00	1.800E−03	3.551E−04	0.005	0.010
LHe in Nose	1.450E−01	1.969E+00	2.190E−02	0.437	0.671
Target Nose	2.700E+00	1.270E−02	2.537E−03	0.038	0.070
4K Shield	2.700E+00	1.300E−03	2.596E−04	0.003	0.007
LN_2 Shield	2.700E+00	3.800E−03	7.610E−04	0.010	0.021
Scat. Chamber	2.700E+00	5.080E−02	1.015E−02	0.165	0.282
Helium Bag	1.786E−04	1.709E+02	2.342E−03	0.057	0.087
Kapton Window	1.420E+00	2.540E−02	2.839E−03	0.044	0.080
Total After			7.106E−02	1.325	2.096

Table 7: Energy loss before and after scattering for the thin g2p production target.

material	X_0	ρ	$\bar{X}_0$	ℓ	t	**fraction of tot**
	g/cm^2	g/cm^3	cm	cm	–	–
Beryllium Window	65.1900	1.848E+00	3.528E+01	3.810E−01	1.081E−03	0.0761
Helium Bag	94.3224	1.786E−04	5.281E+05	7.620E+00	1.443E−05	0.0010
Scat. Chamber	24.0112	2.700E+00	8.893E+00	1.780E−02	2.002E−03	0.1410
LN_2 Shield	24.0112	2.700E+00	8.893E+00	3.800E−03	4.284E−04	0.0302
4K Shield	24.0112	2.700E+00	8.893E+00	1.300E−03	1.462E−04	0.0103
Target Nose	24.0112	2.700E+00	8.893E+00	1.270E−02	1.428E−03	0.1006
LHe in Nose	94.3224	1.450E−01	6.505E+02	4.369E−01	6.716E−04	0.0473
^{12}C disc	42.6969	2.267E+00	1.883E+01	1.588E−01	8.429E−03	0.5936
Total Before	1.420E−02					
^{12}C disc	42.6969	2.267E+00	1.883E+01	1.588E−01	8.429E−03	0.3850
LHe Target Cup	94.3224	1.450E−01	6.505E+02	2.513E+00	3.863E−03	0.1765
LHe in Nose	94.3224	1.450E−01	6.505E+02	4.369E−01	6.716E−04	0.0307
Target Nose	24.0112	2.700E+00	8.893E+00	1.270E−02	1.428E−03	0.0652
4K Shield	24.0112	2.700E+00	8.893E+00	1.300E−03	1.462E−04	0.0067
LN_2 Shield	24.0112	2.700E+00	8.893E+00	3.800E−03	4.284E−04	0.0196
Scat. Chamber	24.0112	2.700E+00	8.893E+00	5.080E−02	5.712E−03	0.2609
Helium Bag	94.3224	1.786E−04	5.281E+05	1.709E+02	3.236E−04	0.0148
Kapton Window	40.5761	1.420E+00	2.857E+01	2.540E−02	8.889E−04	0.0406
Total After	2.189E−02					

Table 8: Radiation thicknesses before and after scattering for the normal g2p carbon dilution target.

material	ρ g/cm^3	ℓ cm	ξ MeV	mp MeV	dE MeV
Beryllium Window	1.848E+00	3.810E−01	4.803E−03	0.077	0.136
Helium Bag	1.786E−04	7.620E+00	1.044E−04	0.002	0.004
Scat. Chamber	2.700E+00	1.780E−02	3.555E−03	0.054	0.099
LN_2 Shield	2.700E+00	3.800E−03	7.610E−04	0.010	0.021
4K Shield	2.700E+00	1.300E−03	2.596E−04	0.003	0.007
Target Nose	2.700E+00	1.270E−02	2.537E−03	0.038	0.070
LHe in Nose	1.450E−01	4.369E−01	4.860E−03	0.090	0.149
^{12}C disc	2.267E+00	1.588E−01	2.760E−02	0.500	0.770
Total Before			4.448E−02	1.056	1.256
^{12}C disc	2.267E+00	1.588E−01	2.760E−02	0.500	0.770
LHe Target Cup	1.450E−01	2.513E+00	2.796E−02	0.564	0.857
LHe in Nose	1.450E−01	4.369E−01	4.860E−03	0.090	0.149
Target Nose	2.700E+00	1.270E−02	2.537E−03	0.038	0.070
4K Shield	2.700E+00	1.300E−03	2.596E−04	0.003	0.007
LN_2 Shield	2.700E+00	3.800E−03	7.610E−04	0.010	0.021
Scat. Chamber	2.700E+00	5.080E−02	1.015E−02	0.165	0.282
Helium Bag	1.786E−04	1.709E+02	2.342E−03	0.057	0.087
Kapton Window	1.420E+00	2.540E−02	2.839E−03	0.044	0.080
Total After			7.930E−02	1.189	1.896

Table 9: Energy loss before and after scattering for the normal g2p carbon dilution target.

material	X_0	ρ	$\bar{X}_0$	ℓ	t	**fraction of tot**
	g/cm^2	g/cm^3	cm	cm	–	–
Beryllium Window	65.1900	1.848E+00	3.528E+01	3.810E−01	1.081E−03	0.1277
Helium Bag	94.3224	1.786E−04	5.281E+05	7.620E+00	1.443E−05	0.0017
Scat. Chamber	24.0112	2.700E+00	8.893E+00	1.780E−02	2.002E−03	0.2363
LN_2 Shield	24.0112	2.700E+00	8.893E+00	3.800E−03	4.284E−04	0.0506
4K Shield	24.0112	2.700E+00	8.893E+00	1.300E−03	1.462E−04	0.0173
Target Nose	24.0112	2.700E+00	8.893E+00	1.270E−02	1.428E−03	0.1686
LHe in Nose	94.3224	1.450E−01	6.505E+02	4.369E−01	6.716E−04	0.0793
^{12}C disc	42.6969	2.267E+00	1.883E+01	5.080E−02	2.697E−03	0.3185
Total Before	8.469E−03					
^{12}C disc	42.6969	2.267E+00	1.883E+01	5.080E−02	2.697E−03	0.1167
LHe Target Cup	94.3224	1.450E−01	6.505E+02	2.729E+00	4.195E−03	0.1816
LHe in Nose	94.3224	1.450E−01	6.505E+02	4.369E−01	6.716E−04	0.0291
Target Nose	24.0112	2.700E+00	8.893E+00	1.270E−02	1.428E−03	0.0618
4K Shield	24.0112	2.700E+00	8.893E+00	1.300E−03	1.462E−04	0.0063
LN_2 Shield	24.0112	2.700E+00	8.893E+00	3.800E−03	4.284E−04	0.0185
Scat. Chamber	24.0112	2.700E+00	8.893E+00	5.080E−02	5.712E−03	0.2472
Helium Bag	94.3224	1.786E−04	5.281E+05	1.709E+02	3.236E−04	0.0140
Kapton Window	40.5761	1.420E+00	2.857E+01	2.540E−02	8.889E−04	0.0385
Total After	2.310E−02					

Table 10: Radiation thicknesses before and after scattering for the thin g2p carbon dilution target.

material	ρ g/cm^3	ℓ cm	ξ MeV	mp MeV	dE MeV
Beryllium Window	1.848E+00	3.810E−01	4.803E−03	0.077	0.136
Helium Bag	1.786E−04	7.620E+00	1.044E−04	0.002	0.004
Scat. Chamber	2.700E+00	1.780E−02	3.555E−03	0.054	0.099
LN_2 Shield	2.700E+00	3.800E−03	7.610E−04	0.010	0.021
4K Shield	2.700E+00	1.300E−03	2.596E−04	0.003	0.007
Target Nose	2.700E+00	1.270E−02	2.537E−03	0.038	0.070
LHe in Nose	1.450E−01	4.369E−01	4.860E−03	0.090	0.149
^{12}C disc	2.267E+00	5.080E−02	8.832E−03	0.150	0.246
Total Before			2.571E−02	0.424	0.732
^{12}C disc	2.267E+00	5.080E−02	8.832E−03	0.150	0.246
LHe Target Cup	1.450E−01	2.729E+00	3.036E−02	0.615	0.930
LHe in Nose	1.450E−01	4.369E−01	4.860E−03	0.090	0.149
Target Nose	2.700E+00	1.270E−02	2.537E−03	0.038	0.070
4K Shield	2.700E+00	1.300E−03	2.596E−04	0.003	0.007
LN_2 Shield	2.700E+00	3.800E−03	7.610E−04	0.010	0.021
Scat. Chamber	2.700E+00	5.080E−02	1.015E−02	0.165	0.282
Helium Bag	1.786E−04	1.709E+02	2.342E−03	0.057	0.087
Kapton Window	1.420E+00	2.540E−02	2.839E−03	0.044	0.080
Total After			4.776E−02	0.865	1.409

Table 11: Energy loss before and after scattering for the thin g2p carbon dilution target.

material	X_0 g/cm^2	ρ g/cm^3	$\bar{X}_0$ cm	ℓ cm	t –	**fraction of tot** –
Beryllium Window	65.1900	1.848E+00	3.528E+01	3.810E−01	1.081E−03	0.1360
Helium Bag	94.3224	1.786E−04	5.281E+05	7.620E+00	1.443E−05	0.0018
Scat. Chamber	24.0112	2.700E+00	8.893E+00	1.780E−02	2.002E−03	0.2519
LN_2 Shield	24.0112	2.700E+00	8.893E+00	3.800E−03	4.284E−04	0.0539
4K Shield	24.0112	2.700E+00	8.893E+00	1.300E−03	1.462E−04	0.0184
Target Nose	24.0112	2.700E+00	8.893E+00	1.270E−02	1.428E−03	0.1797
LHe in Nose	94.3224	1.450E−01	6.505E+02	4.369E−01	6.716E−04	0.0845
LHe Target Cup	94.3224	1.450E−01	6.505E+02	1.415E+00	2.176E−03	0.2738
Total Before	7.947E−03					
LHe Target Cup	94.3224	1.450E−01	6.505E+02	1.415E+00	2.176E−03	0.1848
LHe in Nose	94.3224	1.450E−01	6.505E+02	4.369E−01	6.716E−04	0.0570
Target Nose	24.0112	2.700E+00	8.893E+00	1.270E−02	1.428E−03	0.1213
4K Shield	24.0112	2.700E+00	8.893E+00	1.300E−03	1.462E−04	0.0124
LN_2 Shield	24.0112	2.700E+00	8.893E+00	3.800E−03	4.284E−04	0.0364
Scat. Chamber	24.0112	2.700E+00	8.893E+00	5.080E−02	5.712E−03	0.4851
Helium Bag	94.3224	1.786E−04	5.281E+05	1.709E+02	3.236E−04	0.0275
Kapton Window	40.5761	1.420E+00	2.857E+01	2.540E−02	8.889E−04	0.0755
Total After	1.177E−02					

Table 12: Radiation thicknesses before and after scattering for the g2p empty dilution target.

material	ρ g/cm^3	ℓ cm	ξ MeV	mp MeV	dE MeV
Beryllium Window	1.848E+00	3.810E−01	4.803E−03	0.077	0.136
Helium Bag	1.786E−04	7.620E+00	1.044E−04	0.002	0.004
Scat. Chamber	2.700E+00	1.780E−02	3.555E−03	0.054	0.099
LN_2 Shield	2.700E+00	3.800E−03	7.610E−04	0.010	0.021
4K Shield	2.700E+00	1.300E−03	2.596E−04	0.003	0.007
Target Nose	2.700E+00	1.270E−02	2.537E−03	0.038	0.070
LHe in Nose	1.450E−01	4.369E−01	4.860E−03	0.090	0.149
LHe Target Cup	1.450E−01	1.415E+00	1.575E−02	0.320	0.483
Total Before			3.263E−02	0.594	0.968
LHe Target Cup	1.450E−01	1.415E+00	1.575E−02	0.320	0.483
LHe in Nose	1.450E−01	4.369E−01	4.860E−03	0.090	0.149
Target Nose	2.700E+00	1.270E−02	2.537E−03	0.038	0.070
4K Shield	2.700E+00	1.300E−03	2.596E−04	0.003	0.007
LN_2 Shield	2.700E+00	3.800E−03	7.610E−04	0.010	0.021
Scat. Chamber	2.700E+00	5.080E−02	1.015E−02	0.165	0.282
Helium Bag	1.786E−04	1.709E+02	2.342E−03	0.057	0.087
Kapton Window	1.420E+00	2.540E−02	2.839E−03	0.044	0.080
Total After			3.949E−02	0.727	1.180

Table 13: Energy loss before and after scattering for the g2p empty dilution target.

material	X_0	ρ	$\bar{X}_0$	ℓ	t	**fraction of tot**
	g/cm^2	g/cm^3	cm	cm	–	–
Beryllium Window	65.1900	1.848E+00	3.528E+01	3.810E−01	1.081E−03	0.1328
Helium Bag	94.3224	1.786E−04	5.281E+05	7.620E+00	1.443E−05	0.0018
Scat. Chamber	24.0112	2.700E+00	8.893E+00	1.780E−02	2.002E−03	0.2458
LN_2 Shield	24.0112	2.700E+00	8.893E+00	3.800E−03	4.284E−04	0.0526
4K Shield	24.0112	2.700E+00	8.893E+00	1.300E−03	1.462E−04	0.0179
Target Nose	24.0112	2.700E+00	8.893E+00	1.270E−02	1.428E−03	0.1753
LHe in Nose	94.3224	1.450E−01	6.505E+02	4.369E−01	6.716E−04	0.0825
Target End Cap	24.0112	2.700E+00	8.893E+00	1.800E−03	1.999E−04	0.0245
LHe Target Cup	94.3224	1.450E−01	6.505E+02	1.414E+00	2.173E−03	0.2668
Total Before	8.145E−03					
LHe Target Cup	94.3224	1.450E−01	6.505E+02	1.414E+00	2.173E−03	0.1815
Target End Cap	24.0112	2.700E+00	8.893E+00	1.800E−03	1.999E−04	0.0167
LHe in Nose	94.3224	1.450E−01	6.505E+02	4.369E−01	6.716E−04	0.0561
Target Nose	24.0112	2.700E+00	8.893E+00	1.270E−02	1.428E−03	0.1193
4K Shield	24.0112	2.700E+00	8.893E+00	1.300E−03	1.462E−04	0.0122
LN_2 Shield	24.0112	2.700E+00	8.893E+00	3.800E−03	4.284E−04	0.0358
Scat. Chamber	24.0112	2.700E+00	8.893E+00	5.080E−02	5.712E−03	0.4771
Helium Bag	94.3224	1.786E−04	5.281E+05	1.709E+02	3.236E−04	0.0270
Kapton Window	40.5761	1.420E+00	2.857E+01	2.540E−02	8.889E−04	0.0742
Total After	1.197E−02					

Table 14: Radiation thicknesses before and after scattering for the g2p dummy dilution target.

material	ρ g/cm^3	ℓ cm	ξ MeV	mp MeV	dE MeV
Beryllium Window	1.848E+00	3.810E−01	4.803E−03	0.077	0.136
Helium Bag	1.786E−04	7.620E+00	1.044E−04	0.002	0.004
Scat. Chamber	2.700E+00	1.780E−02	3.555E−03	0.054	0.099
LN_2 Shield	2.700E+00	3.800E−03	7.610E−04	0.010	0.021
4K Shield	2.700E+00	1.300E−03	2.596E−04	0.003	0.007
Target Nose	2.700E+00	1.270E−02	2.537E−03	0.038	0.070
LHe in Nose	1.450E−01	4.369E−01	4.860E−03	0.090	0.149
Target End Cap	2.700E+00	1.800E−03	3.551E−04	0.005	0.010
LHe Target Cup	1.450E−01	1.414E+00	1.573E−02	0.319	0.482
Total Before			3.296E−02	0.598	0.978
LHe Target Cup	1.450E−01	1.414E+00	1.573E−02	0.319	0.482
Target End Cap	2.700E+00	1.800E−03	3.551E−04	0.005	0.010
LHe in Nose	1.450E−01	4.369E−01	4.860E−03	0.090	0.149
Target Nose	2.700E+00	1.270E−02	2.537E−03	0.038	0.070
4K Shield	2.700E+00	1.300E−03	2.596E−04	0.003	0.007
LN_2 Shield	2.700E+00	3.800E−03	7.610E−04	0.010	0.021
Scat. Chamber	2.700E+00	5.080E−02	1.015E−02	0.165	0.282
Helium Bag	1.786E−04	1.709E+02	2.342E−03	0.057	0.087
Kapton Window	1.420E+00	2.540E−02	2.839E−03	0.044	0.080
Total After			3.982E−02	0.731	1.189

Table 15: Energy loss before and after scattering for the g2p dummy dilution target.

References

[1] J. Singh, V. Sulkosky, E97-110 Tech. Note, https://userweb.jlab.org/~singhj/docs/radlength_sagdhv130.ps.

[2] Particle Data Group, Atomic and Nuclear Properties of Materials, http://pdg.lbl.gov/2012/AtomicNuclearProperties/.

[3] Y. S. Tsai, Lectures given at Nato Advanced Institute on Electron Scattering and Nuclear Structure at Cagliari, Italy, SLAC-PUB-848 (1970).

[4] William R. Leo, Techniques for Nuclear and Particle Physics Experiments: A How-to Approach. Springer-Verlag, Berlin, Second Revised Edition (1994).

[5] Enrico Fermi, Phys. Rev. **57** 493 (1940).

[6] R. M. Sternheimer, S. M. Seltzer, and M. J. Berge, Atomic Data and Nuclear Data Tables **30** 261 (1984).

[7] M. Huang, E08-027 ELOG Post 172 https://hallaweb.jlab.org/dvcslog/g2p/172 (2012).